Meteorol. Atmos. Phys. 65, 77–91 (1998)

Meteorology and Atmospheric Physics

Indian Institute of Tropical Meteorology, Pune, India

Investigation of Mixed Layer Response to Bay of Bengal Cyclone Using a Simple Ocean Model

S. K. Behera, A. A. Deo, and **P. S. Salvekar**

With 9 Figures

Received April 18, 1997
Revised October 9, 1997

Summary

A simple 1.5 layer reduced gravity transport model is used to understand the influence of a moving tropical cyclone on the upper layer of the Bay of Bengal. The wind stress used to force the model is derived from an idealised cyclone. The model cyclone is considered to be a symmetric vortex with both tangential and radial winds. The cyclone center moves northwestwards between the points 97 E, 8 N and 82 E, 23 N. In the control experiment, the cyclone is allowed to move the total distance in 5 days. The oceanic response is asymmetric in contrast to the symmetric wind forcings. Right bias found in the maxima of model circulation and upper layer thickness deviations, is in agreement with other modelling studies.

Fifteen sensitivity experiments are carried out by varying the intensity, size and speed of the cyclone, by changing the model parameters and with different initial conditions. Model fields show linear response to changes in the intensity and size of the cyclone. The changes in the maximum wind of the cyclone produces highest variability in the model fields. Increase in model resolution in association with the corresponding decrease in viscosity results in the enhancement of maxima of the flow magnitude and ULTD. Increasing the phase speed of the initial mode results in a wider spreading of energy and hence decrease in the flow intensity and the upper layer deviations. Model results do not show much variation by considering different initial conditions.

1. Introduction

The tropical cyclones constitute one of the most destructive natural disasters that affect many countries around the globe and cause tremendous loss of lives and property. About 80 tropical cyclones develop over the tropical oceans each year and the Bay of Bengal experiences on an average 4–5 tropical cyclones per year. These cyclones move at speeds of about 6 m/s, with maximum wind speed of 20 m/s, which sometimes reach upto 40 m/s in the case of severe cyclonic storm. Most of the Bay storms, travel towards northwest and strike the coast of Tamilnadu and Andhra Pradesh, i.e. the southeast coast of India. Certain storm takes a northerly direction and make landfall on the coast of Orissa and West Bengal. Sometimes, they recurve and hit the coasts of Bangladesh and Myanmar. Tropical cyclones force a vigorous response in the ocean; surface wave heights in excess of 20 meters and upper ocean current strength of 1 m/s are common features.

The substantial impact of mixed layer heat content and SST, on the genesis and intensification of tropical cyclones, has long been recognized. Both theoretical and numerical models also indicate the great sensitivity of maximum storm intensity to SST (DeMaria and Kaplan, 1994). Tropical cyclone modelling efforts in the past have been mainly concerned with perplexing problems of convective parameterisation, vortex movement and vortex flow interactions (DeMaria, 1985; Greatbatch, 1983, 1984 and Thu and

Krishnamurti, 1992). One of the potentially significant constraints on dynamical predictions of tropical cyclones is the lack of knowledge about the ocean response to the storm forcings. Various observational and numerical studies have shown that tropical cyclone produces significant changes in the underlying ocean thermodynamic structures which also involve SST changes (Nilsson, 1996). Vertical turbulent mixing within the upper oceanic layer and entrainment of cooler thermocline water to the warm mixed layer are the primary mechanisms for SST decrease during the tropical cyclone passage.

Present study deals with the upper mixed layer responses in the Bay of Bengal during the passage of an idealised cyclonic storm, using a simple wind driven reduced gravity ocean model (Behera and Salvekar, 1995). The oceanic influence on the cyclone is not considered for simplicity. The study also deals with the results of sensitivity experiments obtained by changing the model parameters as well as changing the parameters of cyclone such as vortex size, vortex intensity, translation speed, initial conditions, etc.

2. The Model

The model used in this study has one active layer, overlying a deep motionless inactive layer i.e. zero pressure gradient in the lower layer which effectively filters the fast barotropic mode. The model equations are based on vertically integrated shallow water equations over the active layer assuming no vertical shear in horizontal fields. The formulation of the equations and the numerical methods are fully described in Behera and Salvekar (1996). The model equations in Cartesian coordinates are;

$$U_t + (U^2/H)_x + (UV/H)_y - fV + (g'/2)(H^2)_x = A\nabla^2(U) + \tau_{xz}/\rho_1 \quad (1)$$

$$V_t + (UV/H)_x + (V^2/H)_y + fU + (g'/2)(H^2)_y = A\nabla^2(V) + \tau_{yz}/\rho_1 \quad (2)$$

$$H_t + U_x + V_y = w_e \quad (3)$$

Here U and V are zonal and meridional component of vertically integrated upper layer velocity fields, f is the coriolis parameter $(2\Omega \sin\phi)$, H is the upper layer thickness and $g' = g(\rho_2 - \rho_1)/\rho_2$ is the reduced gravity. A is the horizontal eddy viscosity and τ_{xz} and τ_{yz} are the components of the wind stress applied as a body force. Unless specified, the model parameters are $g' = 0.02\,\mathrm{m/s^2}$ and $H_0 = 50\,\mathrm{m}$. These values give an initial gravity wave speed of 1 m/s. The model upper active layer also entrains mass from the lower motionless layer through a source term in the continuity equation as in Chang and Anthes (1978);

$$w_e = \begin{cases} \frac{mu_*^3}{g'H}, & H \le H_{\min} \\ 0, & H \ge H_{\min} \end{cases} \quad (4)$$

where $H_{\min} = 25\,\mathrm{m}$, the efficiency parameter $m = 2.5$ and u_* is the frictional velocity derived from the square root of the wind stress magnitude. This term is included to prevent the surfacing of interface (i.e. $H = 0$). The effect of this entrainment on the upper layer density, momentum and kinetic energy has been neglected. It is assumed that the entrained water (engulfed into the upper layer), has zero velocity and is instantaneously adjusted to the density ρ_1. The horizontal domain used in the model is from 35 E to 115 E and from 24 S to 23 N. Boundary conditions are no slip $(U = V = 0)$ at land boundaries. Modified radiation boundary condition (Camerlengo and O'Brien, 1980) is applied at the open boundaries. This boundary condition allows information to pass through the open boundary, but does not allow to come into the model domain. Except for the high resolution case, the model grid length is ~28 km and the time step is 30 min. In the high resolution case, the grid length is reduced to 7 km and the time step to 20 min. The model is forced only by the surface wind stress derived from the idealised cyclone wind described in the next sub-section. However, the influence of ocean on the cyclone (two way interactions) is not considered in this study.

2.1 The Model Cyclone

The model cyclone assumes a symmetric vortex having tangential and radial winds. The tangen-

Table 1. *Model Parameters for Different Experiments*

Expt No.	Description	V_m (m/s)	R_{max} (km)	Storm speed (m/s)	Duration (days)	A (m^2/s)	Initial mode C_0 (m/s)
1	Control	20	550	4.86	5	1500	1
2	Strong	25	550	4.86	5	1500	1
3	Weak	15	550	4.86	5	1500	1
4	Bigger	20	650	4.86	5	1500	1
5	Smaller	20	450	4.86	5	1500	1
6	Fast	20	550	7.56	3	1500	1
7	Slow	20	550	2.43	10	1500	1
8	High resolution (7 km)	20	550	4.86	5	1500	1
9	High resolution and less viscous	20	550	4.86	5	375	1
10	Low resolution (28 km) Less viscous	20	550	4.86	5	375	1
11	Storm speed $>C_0$	20	550	4.86	5	1500	3, H = 50 m $g' = 0.18$ m/s^2
12	Storm speed $<C_0$	20	550	2.43	10	1500	4, H = 50 m $g' = 0.32$ m/s^2
13	Storm speed $>C_0$	20	550	4.86	5	1500	3, H = 100 m $g' = 0.09$ m/s^2
14	Storm speed $<C_0$	20	550	2.43	10	1500	4, H = 200 m $g' = 0.08$ m/s^2
15	From April	20	550	4.86	5	1500	1.174, H = 100 m, $g' = 0.03$ m/s^2
16	From May	20	550	4.86	5	1500	1.174, H = 100 m, $g' = 0.03$ m/s^2

tial wind $V_\theta(r)$ and the radial wind $V_r(r)$ are considered as follows.

$$V_\theta(r) = \begin{cases} V_m(r/R_{max}), & 0 \le r \le R \\ V_m(R_{max} - r)/(R_{max} - R), & R < r < R_{max} \end{cases} \quad (5)$$

$$V_r(r) = 0.3\, V_\theta(r). \quad (6)$$

where r is the radial distance from the storm center, V_m is the maximum tangential wind at a radial distance R and R_{max} is the maximum radius of the storm. In the main experiment, parameter values of $V_m = 20$ m/s, $R_{max} = 550$ km, and $R = 55$ km are used. However, sensitivity of these parameters is also analysed in several experiments (Table 1). The vortex winds are transformed in the **x** and **y** directions. Constant drag coefficient $C_D = 1.25{*}10^{-3}$ and air density $\rho = 1.2$ kg m^{-3} are then used to compute the wind stress. The storm center is considered to move with a prescribed speed of ~5 m/s, in most of the experiments, except for some sensitivity experiments, where the translation speed is also varied. The center of the storm and the wind stresses are computed at each time step.

3. Results and Discussion

In the control experiment (Exp. 1), the model is integrated for 5 days starting from an initial condition of rest. The wind stress fields derived from the model cyclone are used as input to force the model. The cyclone center moves due northwestward with a speed of 4.86 m/s so that the distance between the points (97 E, 8 N) and (82 E, 23 N) is travelled in exactly 5 days. The results obtained from this experiment are discussed in the next subsection. Some sensitivity experiments are also carried out with various

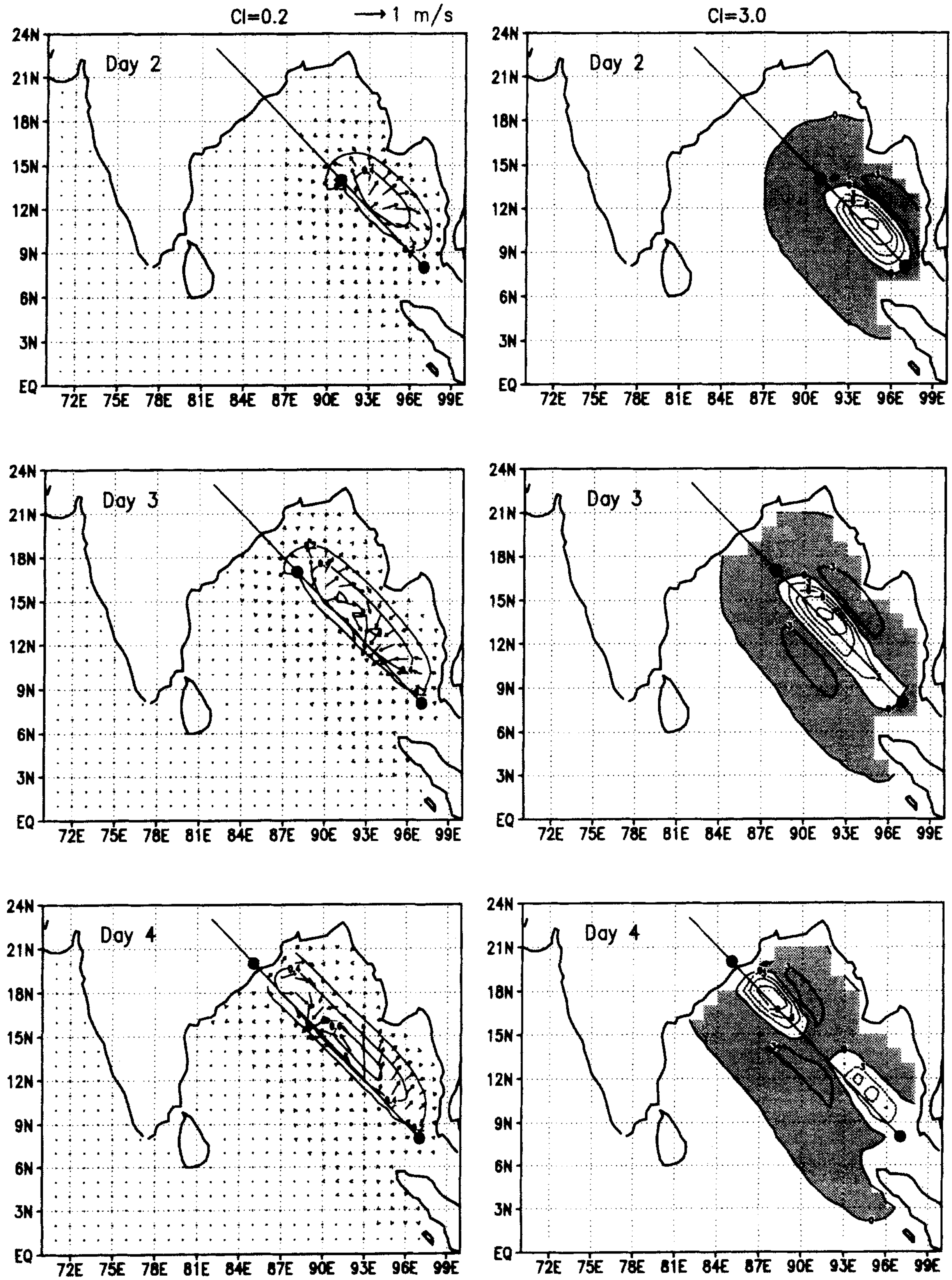

Fig. 1. The model currents (m/s) and upper layer thickness deviations (m) for days 2, 3 and 4 in the control experiment. The initial and present positions of the storm are shown as solid circles on the storm track. The positive ULTD values are shaded. Contour interval is mentioned at the top of the figure

translation speeds of the cyclone and by changing the model parameters (see Table 1). Each experiment is denoted by short description depending on the sensitivity of each parameter. The model fields are stored at 12 hours interval and these instantaneous snap shots are used for the graphics and discussions.

3.1 Control Experiment

The currents and the upper layer thickness deviation (i.e. the deviation of the model upper layer from its initial value) for days 2, 3 and 4 are shown in Fig. 1. These fields are obtained from the snap shots of the middle of the day. The storm track is drawn for easy reference. The initial and current storm center positions are shown as solid circles. Both circulation and model upper layer thickness deviation (ULTD) are asymmetric to the storm center in response to the symmetric wind forcing. The flow is divergent near the storm center and the maximum magnitude of the flow is located right of the storm track. The bias is explained by the sense of rotation on either side of the track with respect to time. The inertial forces turn the ocean currents in the same (opposite) direction of wind stress in the right (left) side of the track. The current maximum at each day lags the storm center by approximately 150 km which can be equivalent to 9 hours with reference to the prescribed cyclone speed. The negative ULTD maximum is also seen right of the track and its center lies behind the prescribed storm center by about 350–400 km i.e. equivalent to 21–24 hrs. It is assumed that the negative (positive) ULTD is an indicator of upwelling (downwelling). The storm center is located over the downwelling region on 2nd and 3rd days. This suggests that in reality, cyclones are probably not affected by the sea surface cooling caused by the upwelling, due to the time lag between storm center and the maximum upwelling region.

Secondary current maxima are seen on day 3 and day 4 at distance of 300–350 km away from the primary current maximum and 500 km from the storm center. The ULTD fields show along track and cross track oscillations. The along track oscillation is clearly envisioned on day 4. These computed results are in good agreement with the other model studies (Chang and Anthes, 1978; Price et al., 1978; Price, 1983). The negative ULTD region oscillates both to the left and right in the wake of the cyclone, however maximum of the negative ULTD is always located to the right of the storm track.

3.2 Sensitivity Experiments with Different Cyclone Radius and Intensity

In this subsection the model results from experiment 2, 3, 4 and 5 are discussed and are compared with those of the control experiment. The model response to the changes in the wind maximum V_m (by 5 m/s) is investigated in experiments 2 and 3 and to the changes in cyclone radius R_{max} (by 100 kms) is investigated in experiments 4 and 5. The time series of ULTD, zonal and meridional current components (**u** and **v**) and wind stress components (τ_{xz} and τ_{yz}) from all these experiments at a point 90 E, 15 N, which lies on the storm track, are shown in the Fig. 2. Maximum variation in model ULT is seen on day 3. The amplitudes of these deviations suggest a linear oceanic response to the changes in the surface forcings. The increase and decrease in the strength of maximum wind V_m, have induced maximum deviations in the model fields. The effect is found to be widespread in space with more (less) region under downwelling in the larger (smaller) radius cases. In all the cases the time lag between the storm center and the maximum deviations in the model fields remains same. This may be due to a smaller deviation in response time as compared to the interval of storing of the model fields which is 12 hrs. The time lags between the wind maxima and the ULTD and current maxima can be clearly seen in the figure.

3.3 Response to Different Storm Speed

Ocean responses to different storm speeds are investigated in the experiments 6 and 7 by approximate 50% increase and decrease in the translation speed, respectively. The translation speed of the storm is 7.56 m/s in the experiment 6, and 2.43 m/s in the experiment 7. Figure 3 shows the current and the ULTD fields from the fast moving storm case after day 1, 2 and 3 and Fig. 4 shows that of the slow moving storm case after day 4, 6 and 8. These particular days are

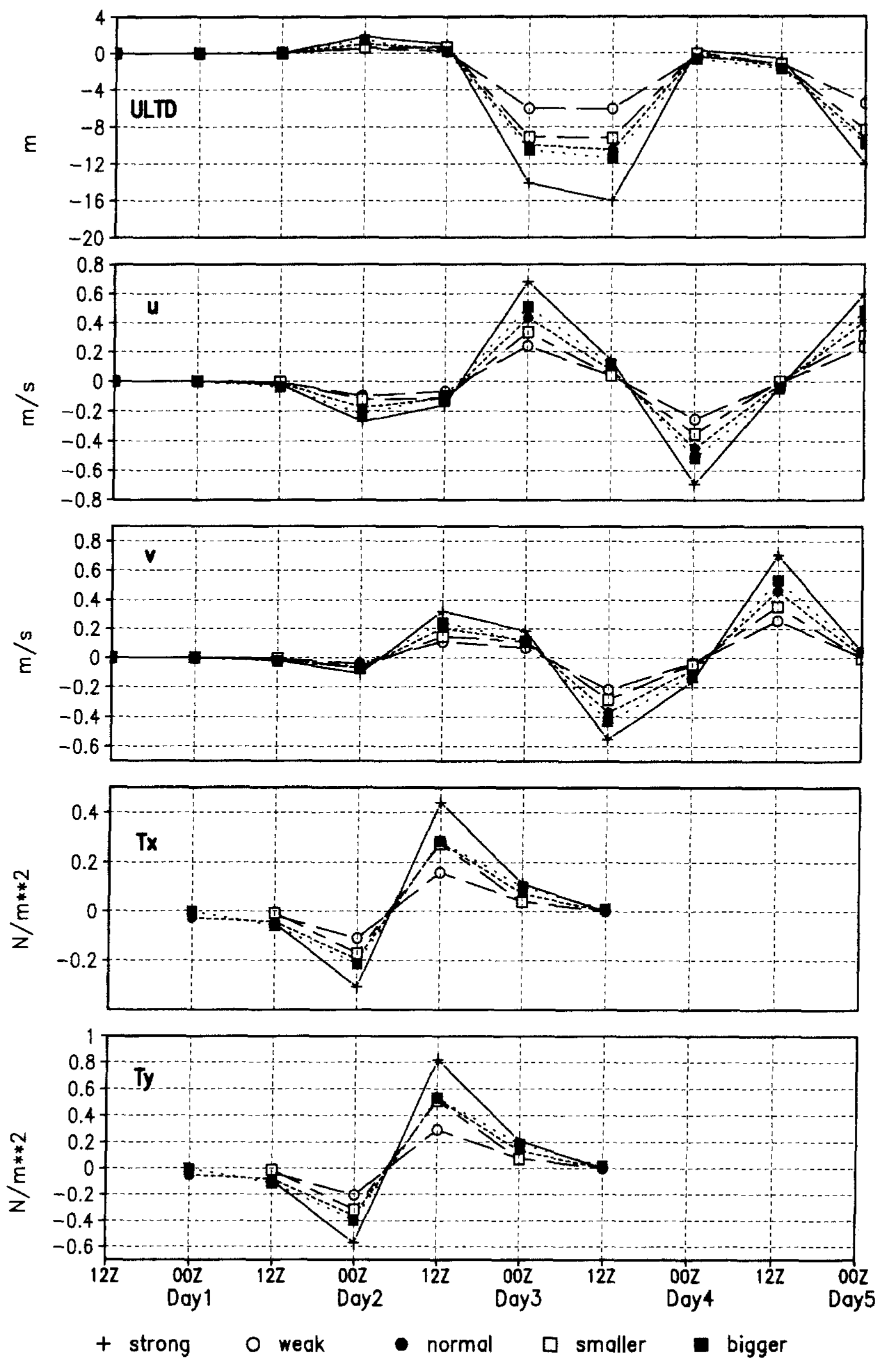

Fig. 2. The time evolution of ULTD, zonal and meridional components of current and wind stress at a point (90 E, 15 N) on the storm track for strong ($V_m = 25$ m/s), weak ($V_m = 15$ m/s), normal (control), smaller ($R_{max} = 450$ km) and bigger ($R_{max} = 650$ km) experiments

specifically chosen for presentation because positions of storm centers on these days and that of the control experiment for 2nd, 3rd and 4th day nearly coincide. The time lags between the storm center and the maximum current divergence and the maximum negative ULTD are increased (decreased) for fast (slow) moving cyclone as compared to the control experiment. In the slow moving case, center of the storm lies over the upwelling region.

The ULTD values are higher in the slow moving case which may be due to the longer duration of mixing. The right bias of the ocean response is slightly more in the case of the fast moving storm. All these results are in close agreement with analytic solutions (Geisler, 1970)

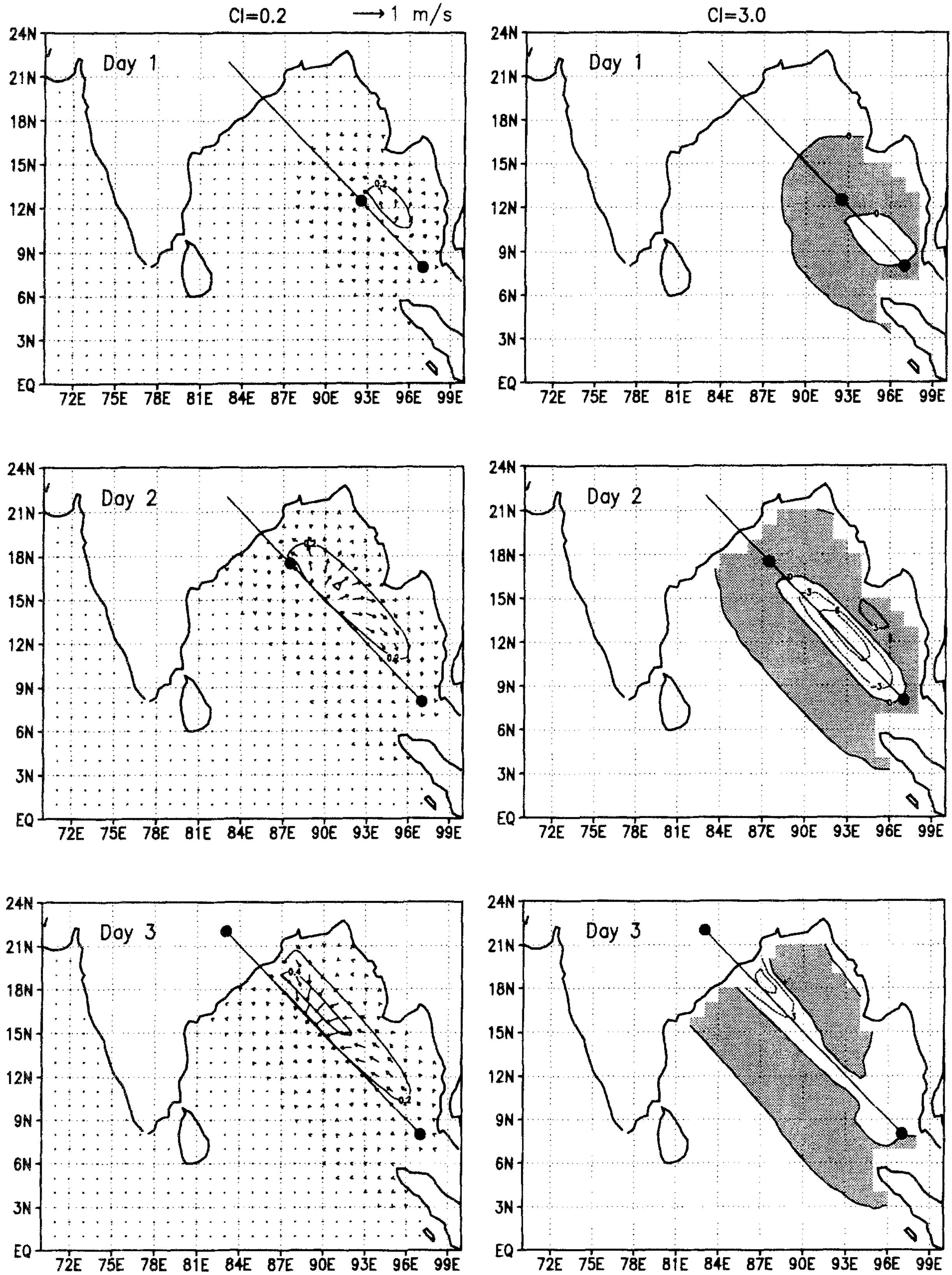

Fig. 3. Same as Fig. 1 but for days 1, 2 and 3 in the fast moving cyclone experiment

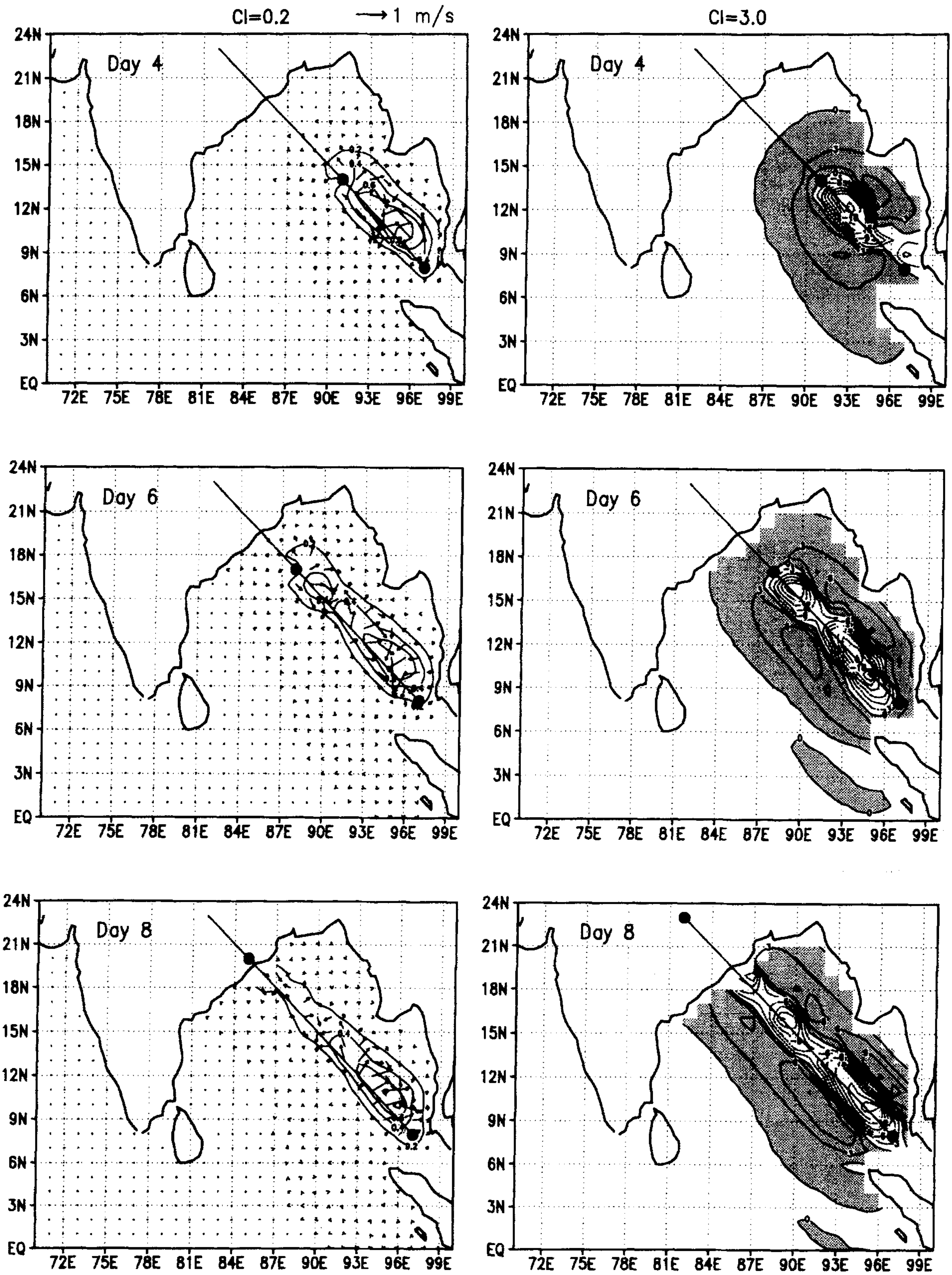

Fig. 4. Same as Fig. 1 but for days 4, 6 and 8 in the slow moving cyclone experiment

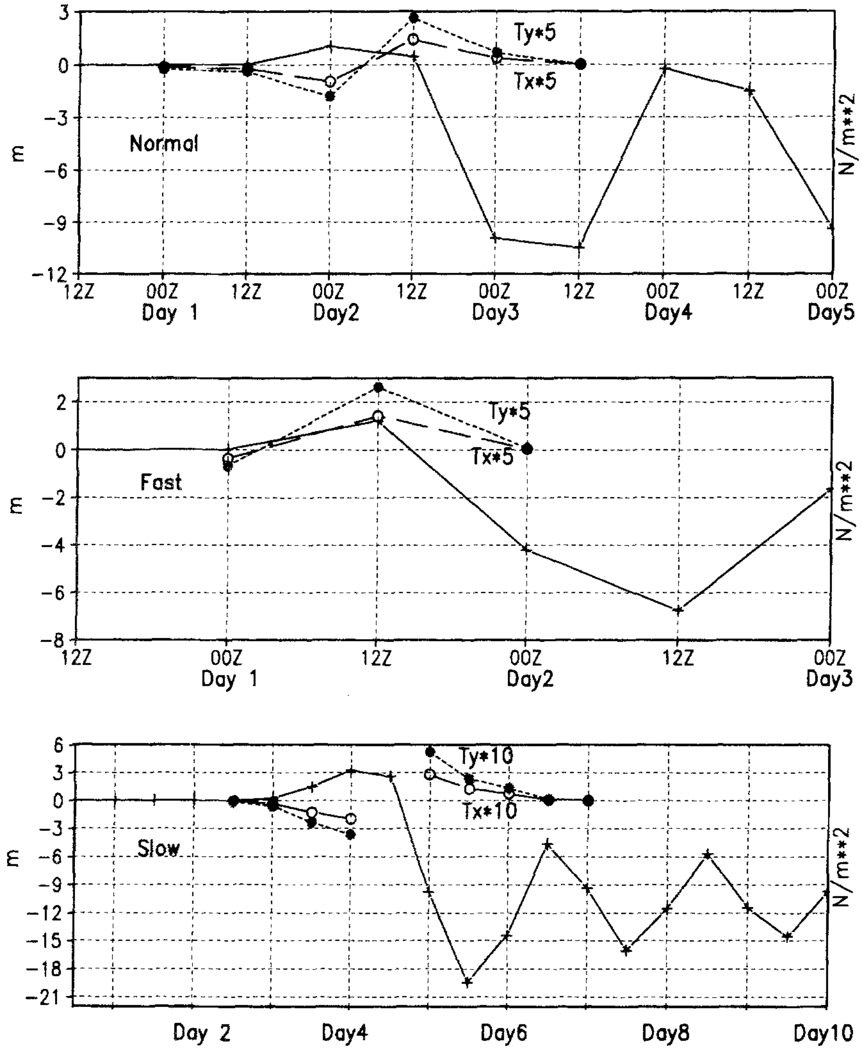

Fig. 5. The time evolution of ULTD (m) at the point (90 E, 15 N) in the control, the fast moving and the slow moving experiments. The zonal and meridional wind stress components (N/m^2) are also shown for comparison. The stress values are scaled by five times in the control and the fast moving experiments and by 10 times in the slow moving experiment

as well as other numerical model results referred earlier. Time series of ULTD and the zonal and meridional components of wind stress at a point 90 E, 15 N for both the cases along with that of the control experiment are shown in the Fig. 5. The differences in time lags between the wind stress fields and the ULTD maxima are clearly seen in this figure. The frequency of the oscillation of the ULTD in the wake of the cyclone is higher in the case of the slow moving cyclone.

3.4 Experiments with Different Model Parameters

The model fields do not show significant changes by increasing the model resolution alone from existing 28 km to 7 km (Exp. 8). However, the wake behind the storm becomes narrow in this case. The resolution is generally increased along with a corresponding decrease in viscosity. In the experiment 9, viscosity is decreased to $375\,m^2/s$ along with the increase in the resolution. The current fields and ULTD fields for the days 2, 3 and 4 are shown in the Fig. 6. The values of maximum ULT deviation and current magnitude are higher in this experiment as compared to the control experiment. Also, more right bias is seen in the high resolution case. Only reducing the eddy viscosity coefficient from $A = 1500\,m^2/s$ to $A = 375\,m^2/s$ and not changing the resolution (Exp. 10) do not show significant variations.

In the experiment 11, the value of the reduced gravity is enhanced nine times to that of the control run i.e. $g' = 0.18\,m/s^2$, to get the initial mode of $C_0 = 3\,m/s$. The model is then integrated for 5 days considering rest of the parameters same as that of the control experiment. Figure 7 shows the velocity and ULTD fields at day 2, 3

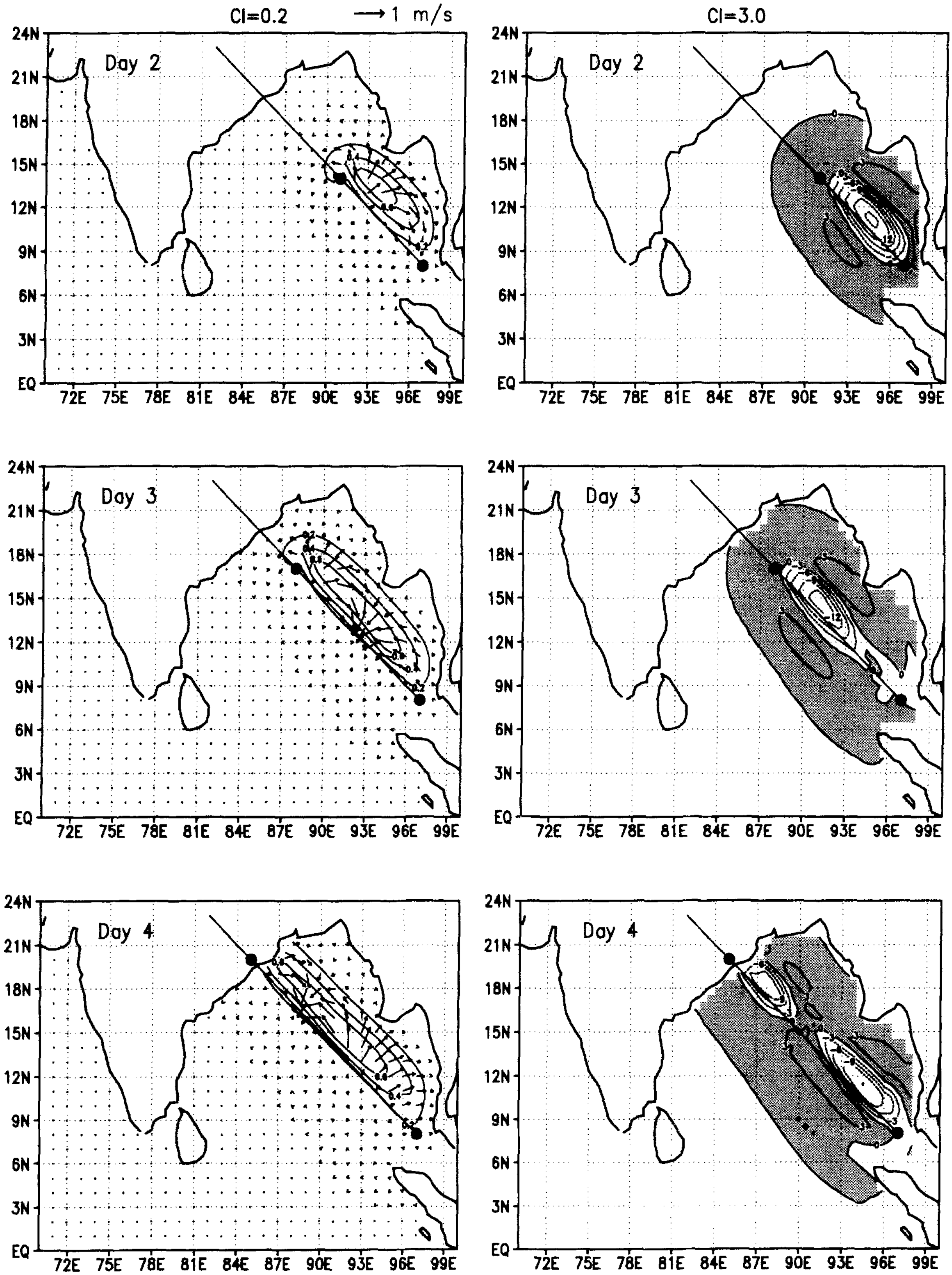

Fig. 6. Same as Fig. 1 but for the high resolution and low viscosity case

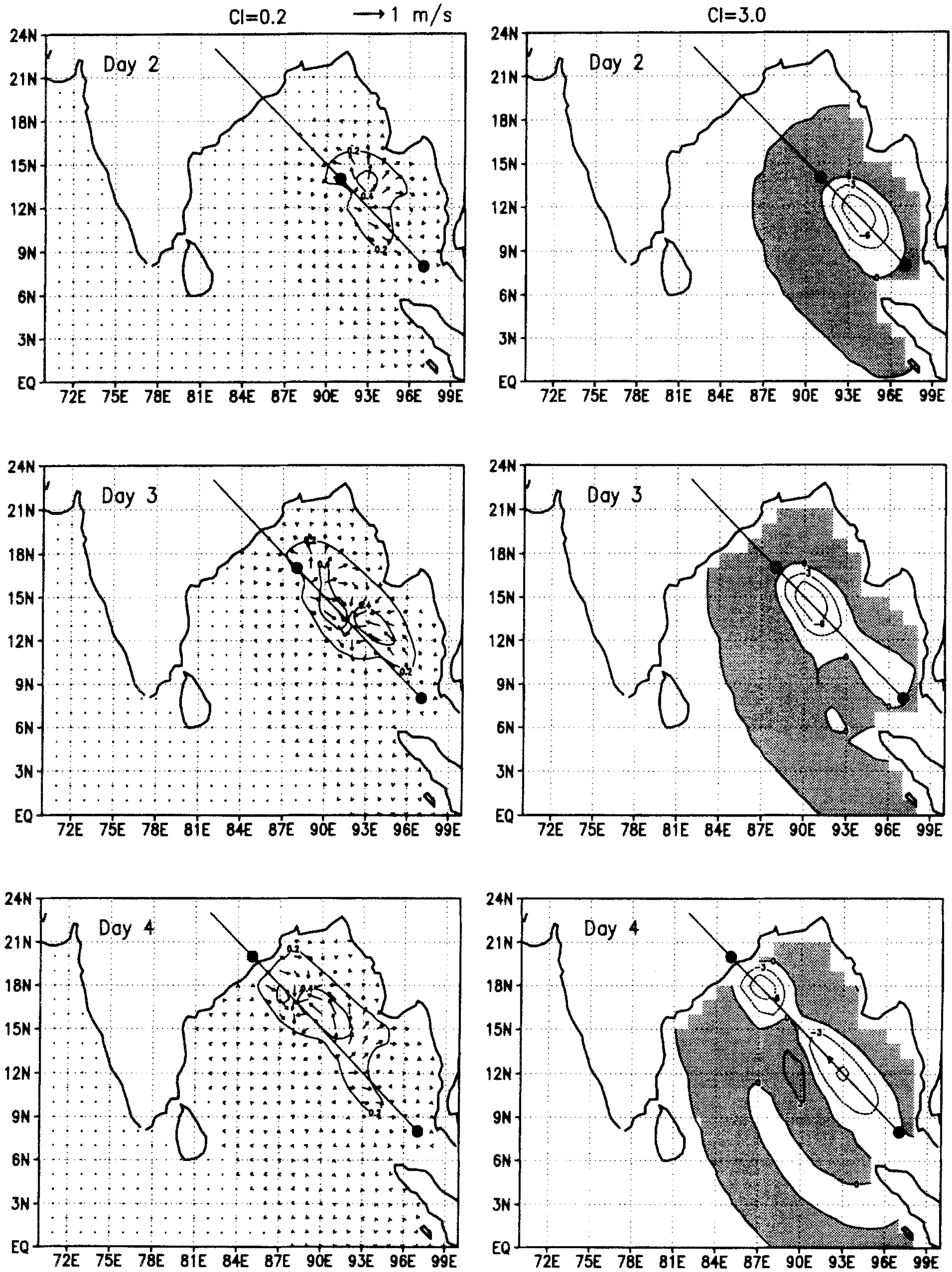

Fig. 7. Same as Fig. 1 but for the case of initial mode $C_0 = 3$ m/s

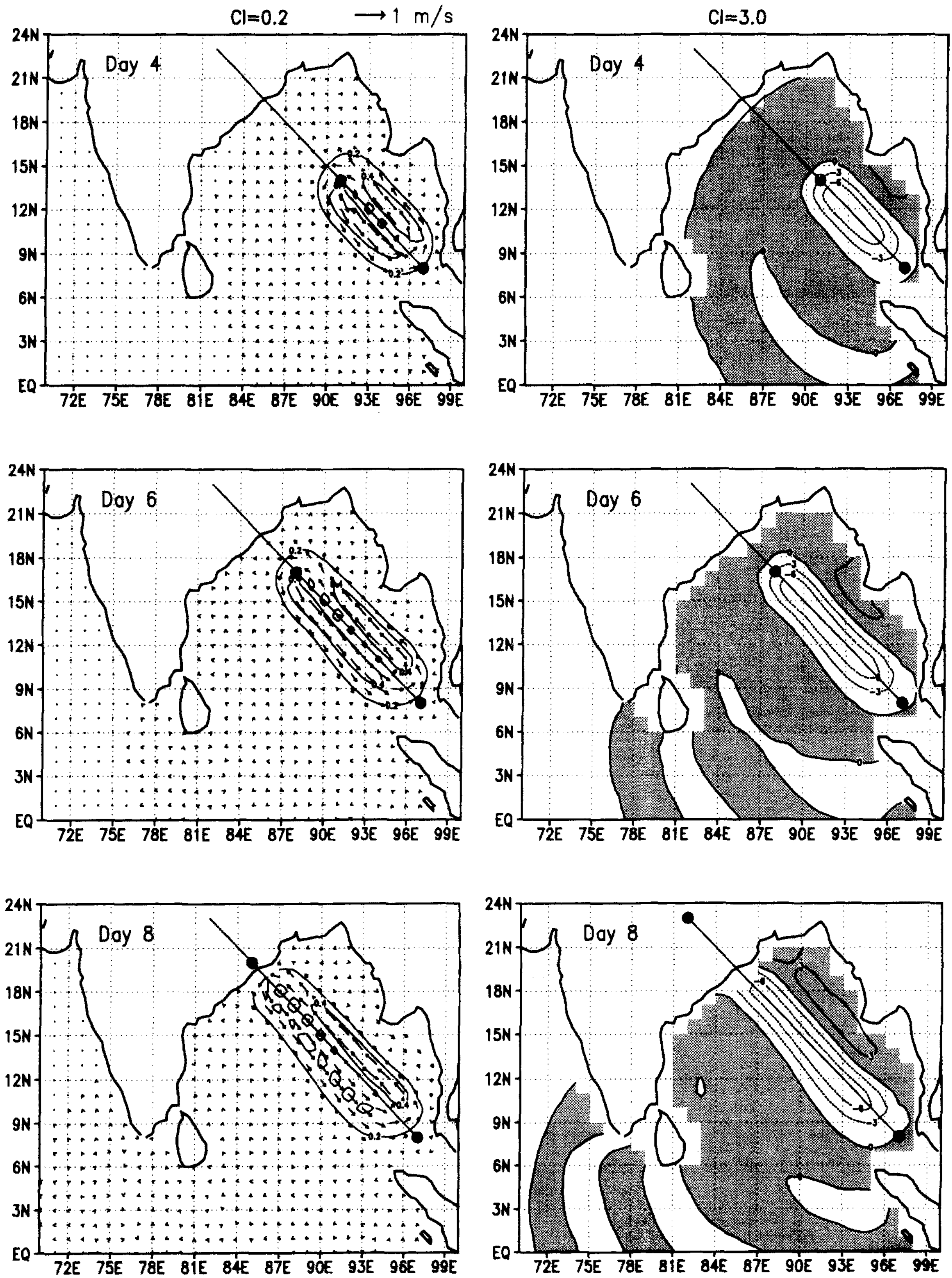

Fig. 8. Same as Fig. 1 but for the case of initial mode $C_0 = 4$ m/s and slow storm speed

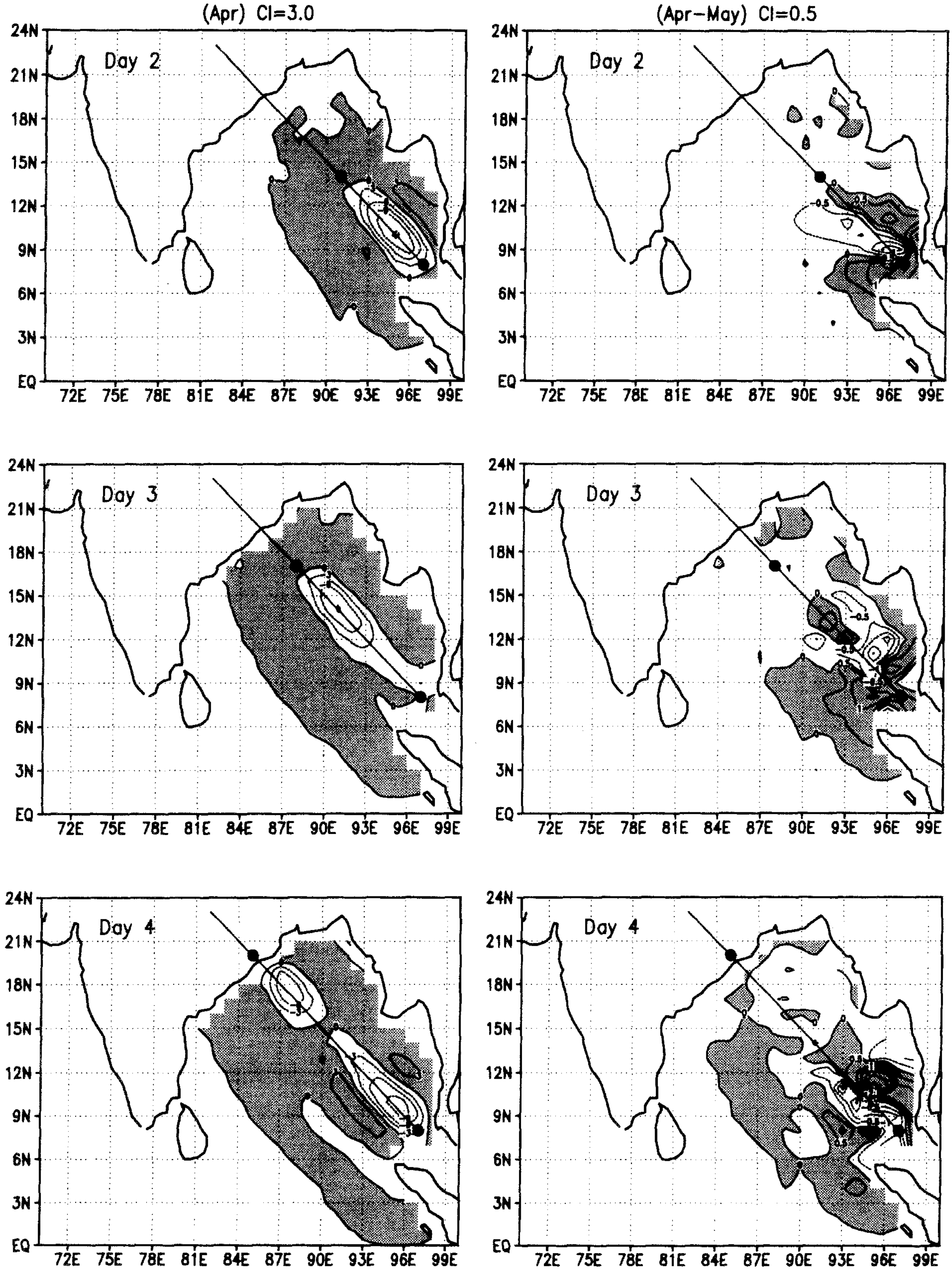

Fig. 9. The ULTD (m) for days 2, 3 and 4 for April initial condition and the difference in ULTD between April and May initial conditions

and 4. Due to the faster initial mode, the model fields spread more westward than the control experiment. However, other model responses remain unchanged. In the experiment 12, the initial mode is increased to $C_0 = 4$ m/s by increasing the value of the reduced gravity $g' = 0.32$ m/s^2. The model is further integrated by considering the storm translation speed of 2.43 m/s, same as the slow moving case. Since the speed of the storm is less than that of the initial mode, the deviation in the model ULT is seen much ahead of the periphery of the storm wind (Fig. 8). Also the westward spread of the model cross track oscillation is much wider as compared to the previous cases. The ULT deviations are seen along west coast of India at day 8, suggesting a remote influence. Experiments 13 and 14 are same as the previous two experiments, except for the higher upper layer initial thickness ($H_0 = 100$ m and 200 m). Parameter values of the reduced gravity are adjusted to obtain the previous two initial modes. The results remain same, except for a decrease in the flow magnitude and ULTD due to a higher initial depth.

3.5 Effect of Initial Condition on the Oceanic Response

In this section, results from the experiments 15 and 16 are discussed. In these experiments the effects of April and May initial conditions on the oceanic responses are investigated. The ocean model was integrated for 10 years to reach an equilibrium condition, with climatological monthly mean winds that are computed from 10 years of FSU pseudostress fields. The model is further integrated for three (four) months to reach April (May) state from January state. The cyclonic vortex is then merged into the April and May mean monthly winds (similar to Thu and Krishnamurti, 1992) as follows.

a) $u^*(r) = u_b(r);\ v^*(r) = v_b(r),\quad \text{for } 0 \le r \le R$

b) $u^*(r) = u_b(r) \cdot (rR_{\max}/R_{\max}R) + u(r) \cdot rR/R_{\max}R;$

$v^*(r) = v_b(r) \cdot (rR_{\max}/R_{\max}R) + v(r) \cdot rR/R_{\max}R,\quad \text{for } R \le r \le R_{\max}$

where, u^* and v^* are data obtained from merging bogus cyclone wind data u_b and v_b into initial data field u and v. The notations rR, $rR_{\max}$ and $R_{\max}R$ represent the distances from r to R, from r to $R_{\max}$ and from R to $R_{\max}$ respectively. These equations show that inside the region R the merged data contains the bogus storm and outside R the interpolated data uses the distances based on the ratio of $rR_{\max}$ and rR. At $r = R$ the merged data set is as the bogus data and at $r = R_{\max}$ the merged data is considered to be the original data to retain the continuity of the winds. The model is integrated for 5 days with these wind forcings from April or May initial conditions. April and May conditions are chosen as the frequency of storms in the Bay of Bengal is generally higher in these premonsoon months. The model is also integrated for 5 days with only April or May winds (without cyclone winds), with the same initial conditions, for comparison of model results. Since, the initial 10 years of model integration was carried out with different parameter values of g' and H_0, those values are retained in these experiments (Table 1). Figure 9 shows the ULTD fields obtained by taking the differences between the ULTD obtained from April initial condition with and without the cyclone winds.

The model results from this experiment do not show much variations from the control experiment. However, the magnitude of ULTD is found lower by 2–4 m on days 3 and 4 than that of the control experiment. The May initial condition has also produced similar results. The differences of the ULTD between the two initial conditions (of April and May) are also shown in the Fig. 9. Deviations in the range of 1–2 m are seen on both the sides of the track. In most of the days more upwelling is inferred to the right of the track for May initial condition case.

4. Conclusions

The simple wind driven reduced gravity model could produce most of the earlier reported analytical and more complex model predicted upper layer responses. The control experiment has shown asymmetric model response to the symmetric wind forcings. The bias to the right of the track in both the maxima of the currents and ULTD is found in the model results. Due to time lag between the storm center and the model response, the storm center always lies ahead of the upwelling region. This probably suggests that in reality, the cyclones are not being affected by the upwelling caused by the intense wind which needs further investigation. The model response to the intensity of the maximum wind and the size of the cyclone is found to be linear. Changes in maximum wind (V_m) cause highest variation in the model fields. Slow moving storms produce stronger model response due to the longer exposure to the storm wind. Increase in the model resolution along with the decrease in viscosity result in intense upwelling and more right bias of the maximum deviations in the model fields. Wider westward spreading of the model ULTD is found by increasing the initial mode. The along track oscillation is found much ahead of the storm when model initial mode is greater than the storm's translation speed. Also, due to the faster westward propagation in this case, ocean responses reach west coast of India in few days, suggesting a remote influence by the cyclone. The initial conditions of April and May are not found to be detrimental in the model responses.

Acknowledgments

Authors are thankful to Director, IITM for his interest in the work. They are grateful to Prof. J. J. O'Brien and Dr. J. N. Stricherz for supplying the FSU wind stress data and to Dr. Brian Doty for GrADS. This work was carried out on the Silicon Graphics Power Challenge computer of the Institute.

References

Behera, S. K., Salvekar, P. S., 1995: A numerical modelling study of the interannual variability in the Indian Ocean. *Mausam,* **46**(4), 409–422.

Behera, S. K., Salvekar, P. S., 1996: Development of simple reduced gravity ocean model for the study of upper North Indian Ocean. IITM Research Report No. RR-072.

Camerlengo, A. L., O'Brien, J. J., 1980: Open boundary conditions in rotating fluid. *J. Comp. Phys.,* **35**, 12–35.

Chang, S. W., Anthes, R. A., 1978: Numerical simulations of the ocean's nonlinear, baroclinic response to translating hurricanes. *J. Phys. Oceanogr.,* **8**, 468–480.

DeMaria, M., 1985: Tropical cyclone motion in a nondivergent barotropic model. *Mon. Wea. Rev.,* **113**, 1199–1210.

DeMaria, M., Kaplan, J., 1994: Sea surface temperature and the maximum intensity of Atlantic tropical cyclone. *J. Climate,* **7**, 1324–1334.

Geisler, J. E., 1970: Linear theory of the response of a two layer ocean to a moving hurricane. *Geophys. Fluid Dyn.,* **1**, 249–272.

Greatbatch, R. J., 1983: On the response of the ocean to a moving storm: The nonlinear dynamics. *J. Phys. Oceanogr.,* **13**, 357–367.

Greatbatch, R. J., 1984: On the response of the ocean to a moving storm: Parameters and scales. *J. Phys. Oceanogr.,* **14**, 59–78.

Nilsson, J., 1996: Mixing in the ocean produced by tropical cyclone. *Tellus,* **48 A**, 342–355.

Price, J. F., Mooers, C. N. K., Leer, J. C. V., 1978: Observation and simulation of storm induced mixed layer deepening. *J. Phys. Oceanogr.,* **8**, 2–599.

Price, J. F., 1983: Internal wave wake of a moving storm: Part I, Scales, energy budget and observations. *J. Phys. Oceanogr.,* **13**(6), 949–965.

Thu, T. V., Krishnamurti, T. N., 1992: Vortex initialization for typhoon track prediction. *Meteorol. Atmos. Phys.,* **47**, 117–126.

Author's address: S. K. Behera, A. A. Deo and P. S. Salvekar, Indian Institute of Tropical Meteorology, Dr. Homi Bhabha Road, NCL Post, Pune 411 008, India.